ORIGINAL PAPER

Oxygen reduction on rotating porous cylinder of modified reticulated vitreous carbon

Mohamed Ismail Awad · Mahmoud M. Saleh ·
Takeo Ohsaka

Abstract A rotating cylinder porous electrode (RCPE) of reticulated vitreous carbon (RVC) matrix was used for oxygen reduction reaction (ORR) in H_2SO_4 solutions. Cyclic voltammetry and hydrodynamic voltammetric techniques were used for electrochemical characterization of the ORR. Cyclic voltammograms in stationary solutions showed better performance of the anodically oxidized RVC (for periods of 1 and 5 min) for the ORR than the untreated RVC in which the first scan (ORR) after the surface treatment was of no utility, and the second scan was presented here. The hydrodynamic voltammograms obtained at the treated RCPE gave well-defined limiting current plateau with positively shifted onset potential as compared with the untreated (plain) RVC electrode. The analysis of the limiting current data on RCPE and the determination of a limiting current enhancement factor α enabled us to quantify the enhancement extent exerted by the anodic oxidation treatment. An enhancement factor of up to ~3 was obtained at the RCPE electrode anodically oxidized for 5 min. It was found that the α slightly decreased with the rotation speed depending on the extent of anodic oxidation of RVC. This was attributed to the different mode of mass transfer (diffusion) to the interior of the micropores with different microstructure resulting from

M. I. Awad · M. M. Saleh · T. Ohsaka (✉)
Department of Electronic Chemistry,
Interdisciplinary Graduate School of Science and Engineering,
Tokyo Institute of Technology,
4259 Nagatsuta, Midori-ku,
Yokohama 226 8502, Japan
e-mail: ohsaka@echem.titech.ac.jp

M. I. Awad · M. M. Saleh
Department of Chemistry, Faculty of Science, Cairo University,
Cairo, Egypt

different extent of anodic oxidation. X-ray photoelectron spectroscopic and scanning electron microscopic measurements helped us to characterize the anodically oxidized RVC surface.

Introduction

Oxygen reduction reaction (ORR) is among the most studied electrochemical reactions because of its importance for power producing devices such as fuel cells [1, 2] and production of valuable chemicals such as hydrogen peroxide [3, 4]. Different electrode materials have been used for the above applications with the aim of reducing the power consumption of the produced H_2O_2 or obtaining lower polarization for the ORR (as a requirement for air batteries and fuel cells) [5–7]. Different electrode configurations such as packed-bed [8], gas diffusion [9], and trickle bed electrodes [10–13] have been used for H_2O_2 production and reviewed recently by Guppta [14]. The rotating cylinder porous electrode (RCPE) offers the advantages of high surface to volume ratio and high rates of mass transfer [15–17]. Walsh et al. [18] studied the mass transfer characteristic of RCPE operating for metal deposition reaction. Electroanalysis using RCPE has been reported by other authors [19, 20].

In previous applications of RVC electrode, the chemical or electrochemical treatment of the RVC electrode was not considered. The electrode was either used as received or after recycling of the electrode potential aiming to obtain reproducible data. Electrochemical oxidation of glassy carbon (GC) electrode has been reported to improve the

electrochemical response of many electroactive species, e.g., dopamine oxidation [21] and oxygen reduction [22]. Although the electrochemical oxidation treatments of planar GC electrode are well documented [23–28], studies on chemical or electrochemical oxidation treatments of RVC are limited, albeit, they are of comparable importance.

The aim of the present work is to study the ORR on RVC electrodes in sulfuric acid solutions. Two electrode setups will be introduced, stationary (flooded) and rotating cylinder porous electrodes. Cyclic and hydrodynamic voltammograms are measured and analyzed to characterize the ORR and its enhancement, which is exerted by anodic oxidation treatment of the RVC electrode. Surface analysis techniques such as scanning electron microscopy (SEM) and X-ray photoelectron spectroscopy (XPS) are used for characterization of the oxidized RVC surface.

Experimental

Electrodes and cell

The RVC blocks were supplied by ERG Materials and Aero Space Corporation, USA. RVC had specific surface area of 40 $cm^2 cm^{-3}$ and a porosity of 0.9. Only one grade of the RVC of 60 PPI (pore per linear inch) was used during the course of this study. The macropore of the RVC has an average diameter of 300 μm, and the thread (surface) has a diameter of about 70 μm. Porous RVC block was cut in cylinder using a hollow cylindrical brass, cork-boring tool. The RVC cylinder had dimensions of 0.35 (diameter) and 0.6 cm height. RVC cylinder was cemented to gold RDE using conducting silver epoxy glue followed by stoving in an oven at 80 °C for 1 h. The H_2SO_4 solution of 200 ml is bubbled with oxygen for at least 30 min to reach the saturation limit, and then O_2 stream was flushed over the H_2SO_4 solution through the measurements to keep the saturation limit. Measurements in O_2-free solutions were achieved by bubbling N_2 gas for 30 min.

Electrochemical measurements

Electrochemical measurements were performed using a BAS 100 B/W electrochemical analyzer. The working electrode and the counter electrode (a platinum spiral wire) were separated by a porous glass. An Ag/AgCl/KCl (sat.) electrode was used as the reference electrode. A conventional three-electrode cell of around 20 ml was used for the cyclic voltammetric measurements. The RCPE measurements were carried out with a ALS/Chi 832A electrochemical analyzer bi-potentiostat (USA)

coupled with a rotary system from Nikko Keisoku (Japan). In this case, the working electrode compartment was 200 ml to eliminate any possible changes in the O_2 concentration during the measurements.

The oxidative treatment of RVC electrode was conducted potentiostatically in a stationary mode at 2 V (vs Ag/AgCl) for specific time periods in 0.1 M H_2SO_4. All the measurements were carried out at 25±1 °C, and deionized water (Milli-Q, Millipore, Japan) was used to prepare all solutions.

Surface techniques

The SEM images of the electrode surface were observed using a scanning electron microscope (Keyence Company, Japan) at an acceleration voltage of 1.5 kV and a working distance of 7.5 mm. RVC electrode of 0.35 (diameter) and 0.6 cm height as mentioned above was oxidized by applying anodic potential of 2 V in 0.1 M H_2SO_4 solution for different periods of time, i.e., 0, 1, 5, and 10 min. The thus-treated RVCs will be herein after termed RVC_{plain}, $RVC_{1\ min}$, $RVC_{5\ min}$, and $RVC_{10\ min}$. The RVC cylinder was then washed with Milli-Q water, dried with hot air, and cut in slices by a sharp blade. The SEM images were then taken for 0.2-cm slices of thickness. XPS measurements of the previously mentioned samples were performed by ESCA3400 electron spectrometer (SHIMADZU) using an unmonochromatized X-ray source with Mg Kα (1253.6 eV) anode.
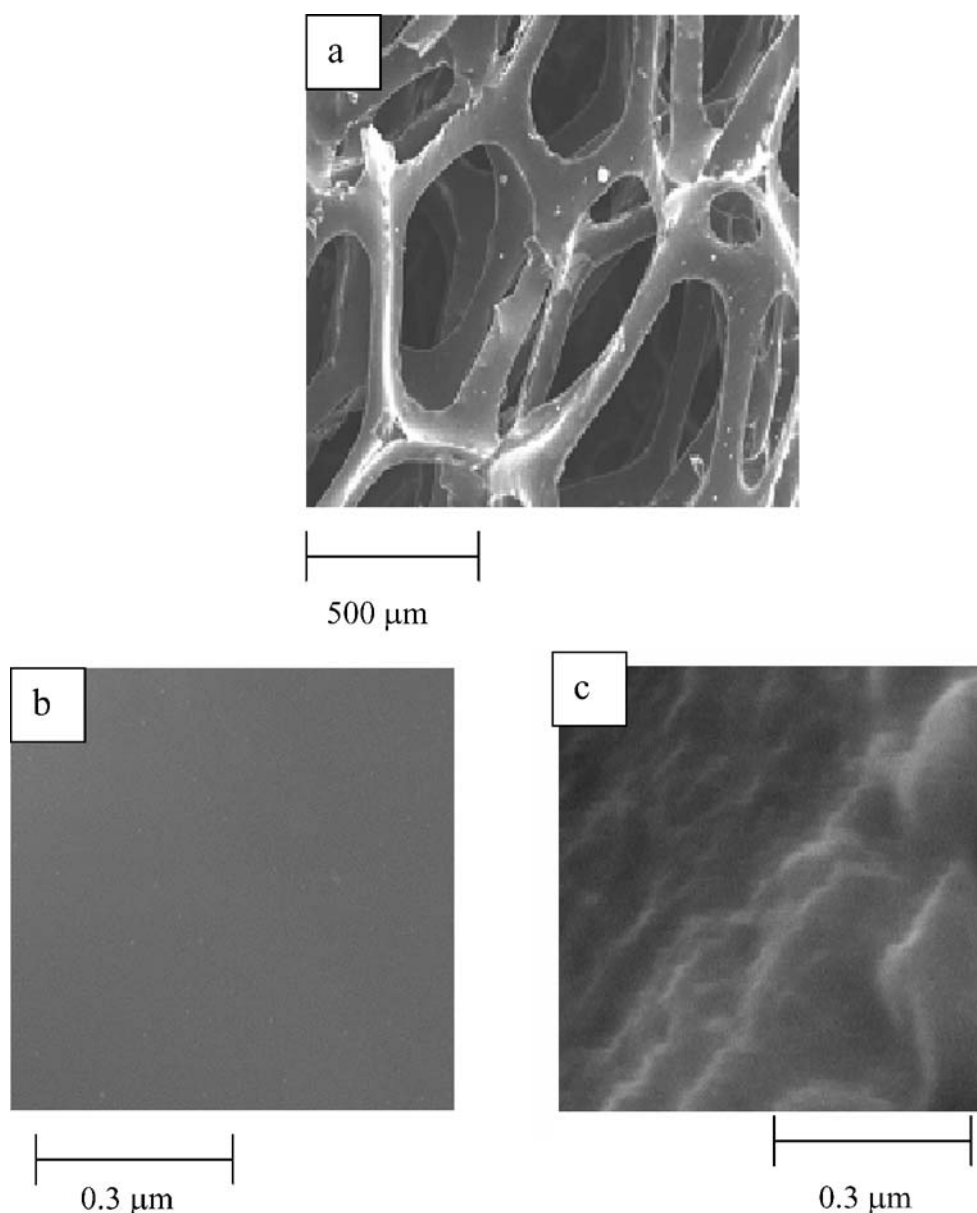
Results and discussion

Results of stationary electrode

The results obtained at the stationary (flooded) RVC electrode are introduced first to show the characterization of the RVC electrode treated by the anodic oxidation process. Oxidation of the electrode was conducted at potential of 2.0 V in 0.1 M H_2SO_4 as described in "Experimental." Current transient for the oxidation process of the electrode was measured for oxidation periods of 1 and 5 min. Current monitoring curves with time during the anodic oxidation of stationary RVC electrodes were similar to those for the oxidation of glassy carbon (GC; data are not shown) [29, 30]. The current-time curves showed an instantaneous increase in current followed by its decrease to some value before reaching a saturation limit. The instantaneous current increase was attributed to the charging of the double layer, and the saturation limit was explained as the activation of the electrode for the water electrolytic oxidation [29, 30].

Surface characterization

Shown in Fig. 1 are the typical SEM images of the plain (Fig. 1a,b) and the oxidized (Fig. 1c) RVC electrodes. The RVC electrode was oxidized for 5 min at 2 V (see "Experimental"). The electrolyte was 0.1 M H_2SO_4 (25 °C). It is quite obvious that the oxidized RVC electrode has a rough surface in contrast to the untreated one. The surface roughness because of anodic oxidation has been often observed for gas chromatography (GC) electrode in acid media by different surface techniques [31]. It has been reported that the surface roughness results from the formation of an oxide layer of graphite, and the layer is responsible for the catalyzed electrochemical reactions of some species [32, 33].

The electrooxidation of GC electrode has been reported to generate different carbon/oxygen functional groups such as phenolic, carbonyl, and carboxylic groups. The different functional groups were usually probed by XPS technique [34]. The XPS spectra of untreated RVC and oxidized RVC were measured to study the effect of the extent of oxidation on the production of possible functional groups by the anodic process (see Fig. 2). XPS has been utilized as an efficient tool for the characterization of GC electrode pretreatment. A wide range of survey spectrum of plain (untreated) RVC sample was taken (data are not shown), and as expected, the spectrum showed only two peaks at binding energies of 284.1 and 532.0 eV, corresponding to carbon and oxygen, respectively, in agreement with the literature [35]. Only short-range spectra for oxygen and

Fig. 1 SEM micrographs obtained for untreated (**a**, **b**) and oxidized (**c**) RVC electrodes. RVC electrode was oxidized by holding the potential at 2.0 V (vs Ag/AgCl) for 5 min in 0.1 M H_2SO_4
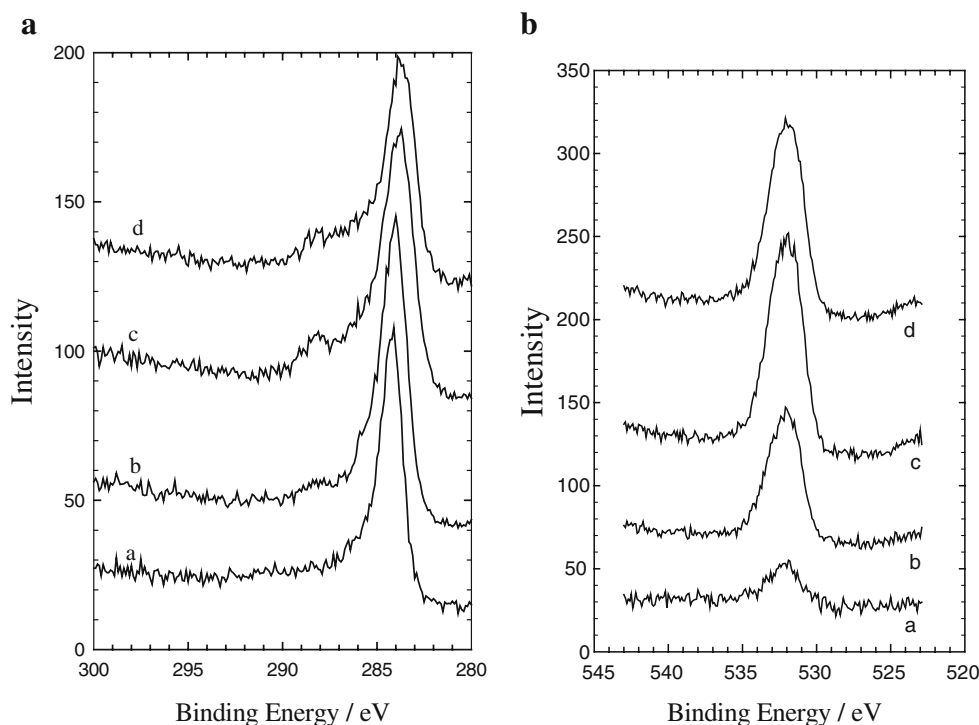
carbon of untreated RVC samples are, respectively, shown in Fig. 2a and b (curves a). The curve fitting of both peaks was performed using the "Asymmetric Gaussian-Lorentzian Formula." The values of the peak intensity of both peaks (for O1s and C1s) were obtained, and the oxygen-to-carbon ratio (φ) was calculated using the following expression [36]:

$$\varphi = \frac{(I_O/S_O)}{(I_O/S_O) + (I_C/S_C)} \tag{1}$$

where I_j and S_j are the peak intensity and the sensitivity factor for carbon (I_C, S_C) and oxygen (I_O, S_O), respectively. The oxygen to carbon ratio for plain RVC was found to be 0.2, which is comparable with the reported values for untreated GC electrode [37, 38].
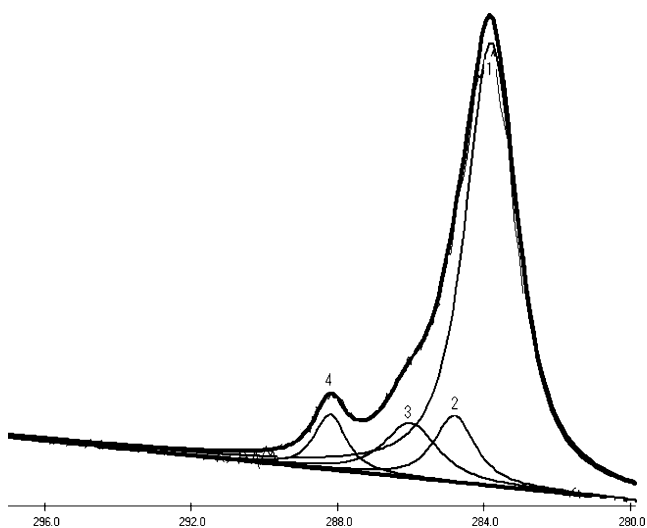
The survey spectrum of the oxidized RVC was similar to that of the untreated sample (data are not shown), and the two peaks corresponding to oxygen and carbon were also observed at the same binding energies as mentioned above for the untreated electrode. Only short-range spectra for the oxidized RVC are given in Fig. 2 (curves b, c, and d). The shape of the oxygen peak, as expected, does not significantly change with the anodic treatment, while that of carbon is significantly changed. Several interesting points can be extracted from Fig. 2:

1. The main peak at 284.2 eV, in addition to the increase in its width at the half-maximum height, is accompanied by another peak at 289 eV and two shoulders at 285.2 and 286.2 eV (see Fig. 2a, curve c). The change in the C1s shape suggests that the environment of the

surface carbon is varied upon electrooxidation, probably reflecting the formation of different surface functional groups generated on anodic oxidation of the electrode [37, 38]. The peak corresponding to carbon was deconvoluted into several Gaussian peaks assigned to different surface functional groups as shown in Fig. 3. The peak at 284.2 eV is ascribed to the graphitic carbon and that at 285.2 to a type of carbon in phenol group. The peak at 286.2 eV is ascribed to carbon in carbonyl functional group and, finally, that at 289 eV corresponds to carbon in the carboxylic group [37]. In this case, the oxygen to carbon ratio (O/C ratio) was calculated using the following equation:

$$\text{O/C ratio} = A_{C-OH} + A_{C=O} + 2 \times A_{COOH} \tag{2}$$

where A_{C-OH}, $A_{C=O}$, and A_{COOH} are the intensity ratios of the different functional groups in the C1s spectrum. The oxygen/carbon ratio was found to be 0.33, which is larger than that (0.2) of the untreated RVC sample (Fig. 2a).

2. While the intensity of the main graphitic peak did not significantly change with the increase in the oxidation time, the intensities of the peak at 289 eV and the two shoulders at 285.2 and 286.2 eV were found to change with different oxidation extent.

3. The peak width of the main peak at 284.2 eV increased with increasing the oxidation time to 5 min and then a little bit decreased on further oxidation.

4. The intensity of the peak corresponding to carbon in carboxylic group increased with increasing the oxida-

Fig. 3 Curve fitting spectra of C1s XPS spectrum of RVC$_{5 min}$ (Fig. 2a, curve c). The peaks *1*, *2*, *3*, and *4* correspond to the graphitic carbon, the carbon in phenol group, the carbon in carbonyl group, and the carbon in carboxylic group, respectively

tion time up to 5 min (Fig. 2a, curve c) and then decreased (Fig. 2a, curve d).

5. The intensity of the O1s peak (Fig. 2b) increased with increasing the time of oxidation and reached a constant value (see Fig. 4).

From the data shown in Fig. 2, the O/C ratios were calculated for the different samples and then plotted against the oxidation time (Fig. 4). The RVC$_{1 min}$ sample resulted in the increase in the O/C ratio from 0.2 (untreated RVC) to 0.24. With increasing the time of oxidation to 5 min, the O/C ratio increased to 0.33. However, further increasing of the time of oxidation did not result in the increase in the O/C ratio.
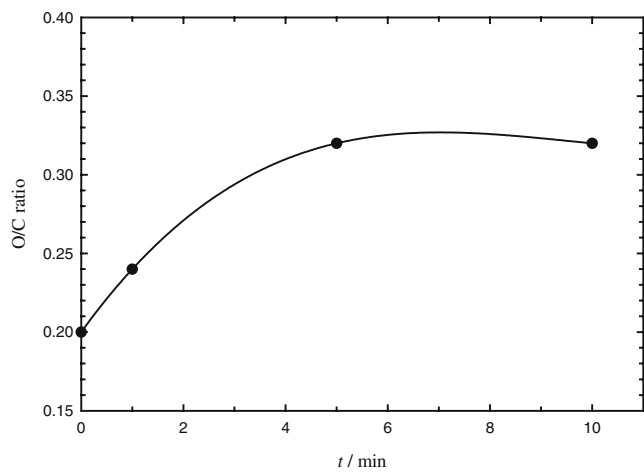
Fig. 4 Plot of the O/C ratio vs the oxidation time

Oxygen reduction

The effects of the surface treatment of the RVC electrode on the ORR are discussed here based on the cyclic voltammograms (CVs) obtained in stationary electrolyte. Figure 5 shows the typical CVs obtained at the untreated and the oxidized RVC electrodes in 0.1 M H$_2$SO$_4$ under N$_2$ or O$_2$ atmosphere. The oxidation at 2 V was applied to RVC electrode at stationary conditions, i.e., flooded assembly in 0.1 M H$_2$SO$_4$ for different time periods. The background current at the oxidized RVC electrode (curve d$'$) under N$_2$ atmosphere is more pronounced than that at
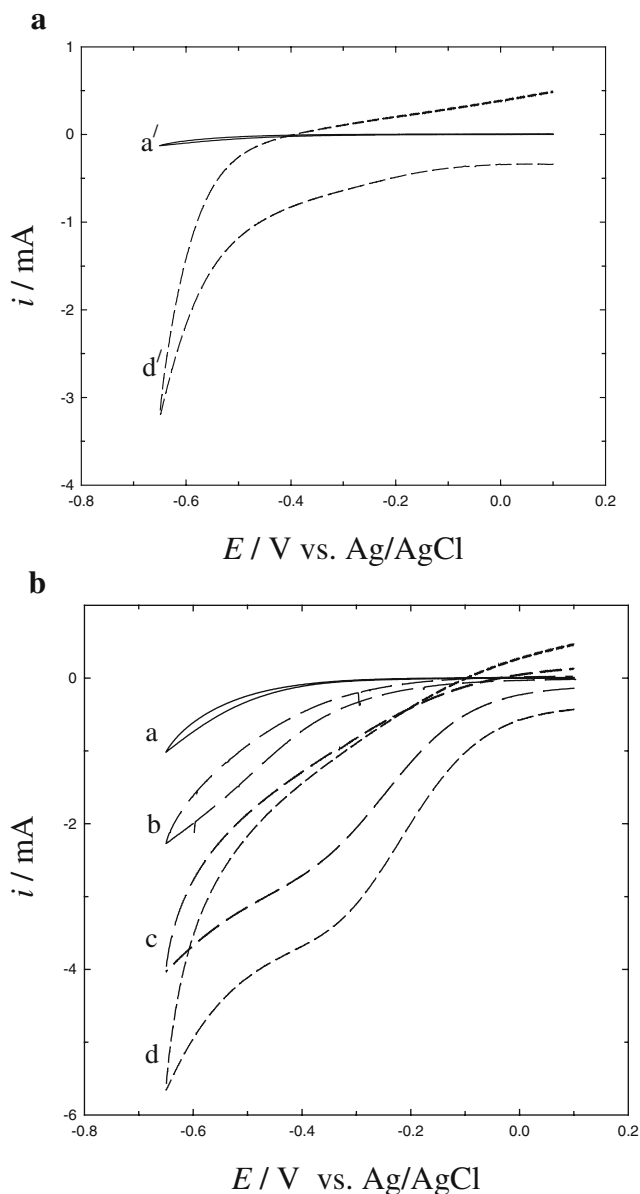
Fig. 5 CVs obtained at *a* RVC$_{plain}$, *b* RVC$_{1 min}$, *c* RVC$_{2 min}$, and *d* RVC$_{5 min}$ electrodes in O$_2$-saturated 0.1 M H$_2$SO$_4$ at scan rate of 20 mV/s (**b**). Voltammograms *a$'$* and *d$'$* were obtained at RVC$_{plain}$ and RVC$_{5 min}$ electrodes, respectively, in N$_2$-saturated 0.1 M H$_2$SO$_4$ solution (**a**)

the untreated electrode (curve a'). The features of the CVs for the ORR in Fig. 5b are highly dependent on the time of anodic oxidation. At the plain RVC (curve a), the oxygen reduction peak is largely obscured by the hydrogen evolution reaction, and thus, it is ill-defined. The ORR at the oxidized RVC is shifted to more positive potential depending on the oxidation time. The most positive shift in the ORR was observed at the $RVC_{5\ min}$ electrode. Longer oxidation of RVC electrode (CVs are not shown here) gave a high background current (capacitive current) and resulted in a distorted CV. Within the studied time range, the ORR current increased as the time of oxidation was increased. A relatively well-defined limiting current plateau for the ORR was observed at the $RVC_{5\ min}$ electrode (curve d). It is worthwhile to mention that the CVs shown in Fig. 5 were obtained at the second scan. The first scan of potential from 0.1 V to the negative direction of potential in O_2-saturated

H$_2$SO$_4$ (also in N$_2$-saturated H$_2$SO$_4$) resulted in a broad peak. The potential of this peak was found to depend on the extent of oxidation. This broad peak was considered to correspond to the reduction in the oxide layer formed upon electrooxidation of the electrode. Similar behavior was previously reported [39] for GC electrode.

It is also noteworthy to mention that the voltammetric behavior of the oxidized RVC was quite stable as long as the potential is not scanned to far negative value, i.e., as long as no intensive hydrogen evolution is carried out at the electrode for long time. The oxidized RVC electrode catalyzes both the ORR and hydrogen evolution reaction (HER). The hydrogen evolution enhancement is evident from the CVs recorded in the O$_2$-free electrolyte as shown in curves a′ and d′ (Fig. 5a). This can be attributed to the surface functionalization, especially the formation of carbon-oxygen functional groups on the RVC surface, which becomes prominent as the extent of oxidation is increased (as discussed above based on the XPS data), of the electrode surface. The same reason could be behind the positive shift in the onset potential of the ORR on increasing the extent of oxidation of the RVC electrode. The formation of quinone functional groups on the surface of the oxidized planar GC electrode has been reported to enhance the ORR [40]. The increased limiting current for the ORR at oxidized RVC may be attributed to the change in the surface roughness as was revealed from SEM images (see Fig. 1) Therefore, a remarkable impact of RVC oxidation on the ORR can be expected: Increasing the oxidation time increases the extent of the formation of surface functional groups, which may be reflected on the catalyzed ORR. However, when the $RVC_{5\ min}$ and $RVC_{10\ min}$ electrodes were compared, there was no significant difference in the ORR peak current. This can be explained in the light of the O/C ratios extracted from the XPS measurements (see Fig. 4), that is, the O/C ratios were almost the same at these both RVC electrodes. Electrooxidation of GC has been reported to be a possible way of desorption to some impurities that may be introduced in the mechanical polishing step and, consequently, to increase the activity of the electrode [30]. It can also affect the specific chemical interactions associated with the electrochemical reaction, such as adsorption or change in hydration of the electroactive species, and therefore, it may catalyze some electrochemical reactions [30].

Results of the RCPE

Figure 6a,b shows the hydrodynamic voltammograms for the ORR at the RCPEs of RVC$_{plain}$ and RVC$_{1\ min}$ in 0.1 M H$_2$SO$_4$, respectively. Similar results were obtained at RVC$_{5\ min}$ (data are not shown). Background corrections (mainly related to the hydrogen evolution) were made on all
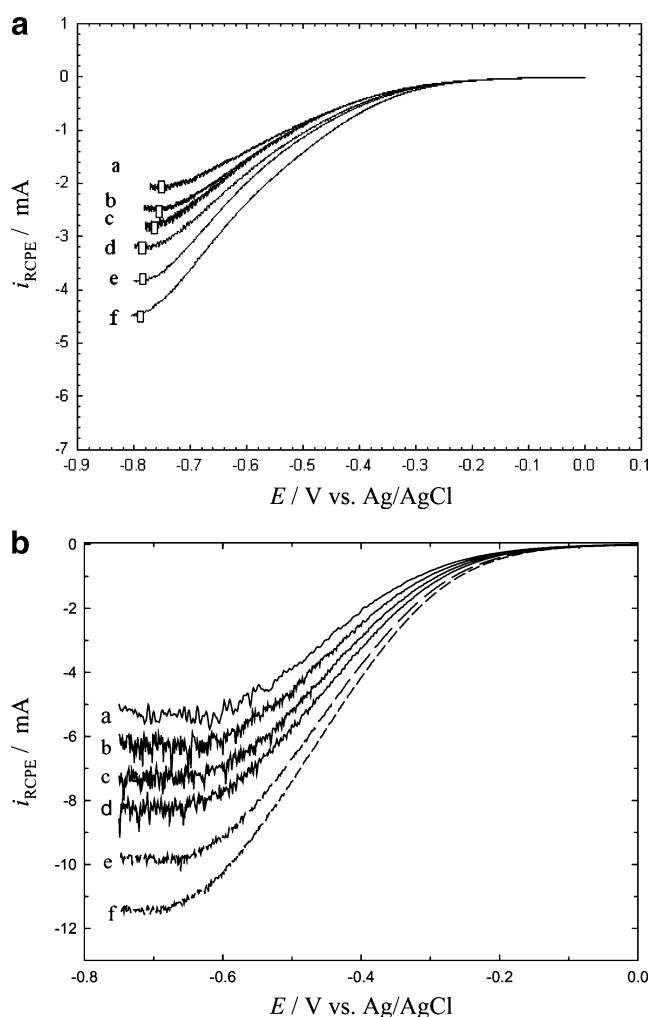
Fig. 6 Hydrodynamic voltammograms at **a** RVC$_{plain}$ and **b** RVC$_{1\ min}$ in O$_2$-saturated 0.5 M H$_2$SO$_4$ solution at different rotation rates: (*a*) 400, (*b*) 600, (*c*) 800, (*d*) 1,000, (*e*) 1,500, and (*f*) 2,000 rpm. Potential Scan rate, 20 mV s^{-1}. The *squares* point to the positions of the limiting currents
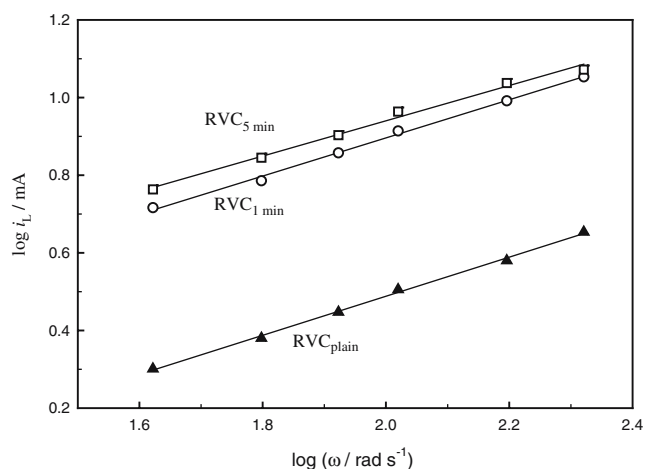
Fig. 7 Log–Log plots of i_L vs ω for the ORR at RVC$_{plain}$, RVC$_{1\ min}$, and RVC$_{5\ min}$ electrodes in O$_2$-saturated H$_2$SO$_4$ solution

the voltammograms by measuring the current of the hydrogen evolution reaction at the individual electrodes in O$_2$-free 0.1 M H$_2$SO$_4$ solution. At a glance, we can see a positive shift in the onset potential of the ORR at the oxidized RVC electrodes as in the CVs obtained at the stationary RVC electrodes (see Fig. 5).

The hydrodynamic voltammograms for the ORR at the oxidized RVC (Fig. 6b) have well-defined limiting current plateaus, and hence, the limiting currents were estimated at $E=-0.7$ V. On the other hand, the limiting currents for the untreated electrode (Fig. 6a) were determined at potentials at which semiplateaus were observed (indicated by the open squares on the voltammograms). The limiting currents obtained in Fig. 6a,b can be correlated to the rotation speed (ω) by the following empirical correlation [41];

$$i_L = a\omega^b \tag{3}$$

where a and b are constants. Figure 7 shows double logarithmic plots of the limiting current, i_L vs the rotation speed for the three electrodes: plain and 1- and 5-min oxidized RVC electrodes. The slopes of the linear plots were calculated using a linear least-squares regression. The obtained line equations and their correlation coefficients are given in Table 1.

The enhancement of the ORR resulting from the anodic oxidation treatment of RVC can be further quantified by

Table 1 Line equations and their correlation coefficients for the different electrodes

| Electrodes	Equations	Correlation coefficient
RVC$_{plain}$	$i_L=0.303\omega^{0.504}$	0.998
RVC$_{1\ min}$	$i_L=0.820\omega^{0.491}$	0.997
RVC$_{5\ min}$	$i_L=0.931\omega^{0.454}$	0.992

considering the limiting current enhancement factor, α. This factor can be given by;

$$\alpha = \frac{i_{L,\ oxidized\ RVC}}{i_{L,\ plain\ RVC}} \tag{4}$$

where $i_{L,oxidized\ RVC}$ and $i_{L,plain\ RVC}$ are the limiting currents for the ORR at the oxidized and plain (untreated) RVC electrodes, respectively. Shown in Fig. 8 are plots of the limiting current enhancement factor α vs the rotation speed for the RVC$_{1\ min}$ and RVC$_{5\ min}$ electrodes. The α values are 2.5–2.6 and 2.5–2.9 at the RVC$_{1\ min}$ and RVC$_{5\ min}$, respectively. They decrease with increasing rotation speed. This may be attributed to the diffusion limitation of the O$_2$ molecules inside the micropores (microstructure) induced by the anodic oxidation treatment. It is noteworthy to mention that the RCPE is favorable when a high sensitivity is needed. Thus, the RCPE finds its way in electroanalysis and the removal of some contaminants from dilute solutions [42, 43]. In the present case, the enhancement of the ORR (yielding H$_2$O$_2$) is considered to be achieved as a combined result of the high mass-transfer effect and the large specific surface area of the RCPE of the anodically oxidized RVC.

Summary and conclusions

The article was dedicated to characterize an anodically oxidized RVC electrode by surface analysis techniques and also by testing the effect of the anodic oxidation treatment on the electrocatalysis for the ORR in acid solutions. Two electrode systems were used, mainly, stationary (flooded) electrode and rotating cylinder porous electrode (RCPE) made of RVC matrix. SEM showed the surface roughness, and XPS probed the extent of the surface modification (formation of surface functional groups) exerted by the anodic oxidation of the RVC electrode in 0.1 M H$_2$SO$_4$.
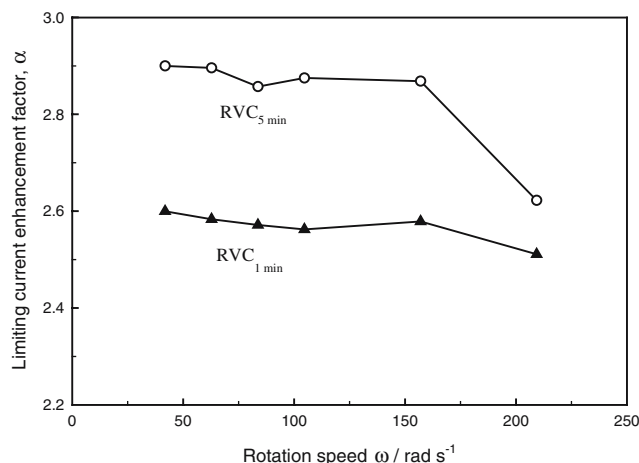
Fig. 8 Current enhancement factor (α) vs rotation speed (ω) for the ORR at RVC$_{1\ min}$ and RVC$_{5\ min}$ electrodes in O$_2$-saturated H$_2$SO$_4$

The surface modification resulted in an enhancement of the ORR, i.e., a positive shift of the onset potential and an increase in the limiting current of the ORR. An enhancement factor α was found to be 2.5–2.9, depending on the extent of the anodic oxidation treatment. The results showed that the RCPE of anodically treated RVC can be used to significantly electrocatalyze the ORR, and this study opens the new area for production of H_2O_2 at higher rates.

References

1. Xu H, Song Y, Kunz H, Fenton J (2005) J Electrochem Soc 152:A 1828
2. Mukerjee S, Srinivasant S, Appleby A (1993) Electrochim Acta 38:1661
3. Qiang Z, Chang J, Huang C (2002) Water Res 36:85
4. Pozzo A, Di Palma L, Merli C, Petrucci E (2005) J Appl Electrochem 35:413
5. Do J, Chen C (1994) J Appl Electrochem 24:936
6. El-Deab M, Ohsaka T (2002) Electrochem Commun 4:288
7. Raj C, Abdelrahman A, Ohsaka T (2005) Electrochem Commun 7:88
8. Sadoh M, Kodera T, Ichino T (1991) J Chem Eng Jpn 24:165
9. Brillas E, Alcaide F, Cabot P (2002) J Electrochem Soc 149:E64
10. Guppta N, Oloman C (2006) J Appl Electrochem 36:255
11. Oloman C, Watkinson A (1997) J Appl Electrochem 9:117
12. Sadoh M, Yamamoto M, Kawamoto T, Okajima K, Yamada N (2001) J Chem Eng Jpn 34:884
13. Yamada N, Yaguchi T, Otsuka H, Sadoh M (1999) J Electrochem Soc 146:2587
14. Guppta N (2004) PhD thesis, University of British Coulombia, Vancouver BC, Canada
15. Reade G, Bond P, de Leaon C, Walsh F (2004) J Chem Technol Biotechnol 79:946
16. Friedrich J, de-Leon C, Reads W, Walsh F (2004) J Electroanal Chem 561:203
17. Gyenge E, Oloman C (2003) J Appl Electrochem 33:665
18. Reade G, de-Leon C, Friedrich J, Walsh F (2006) Electrochim Acta 51:2728
19. Blaedel W, Wang J (1980) Anal Chem 52:1697
20. Blaedel W, Wang J (1980) Anal Chem 52:76
21. Nagaoka T, Fukanage T (1988) Anal Chem 160:2766
22. Vaqik K, Schiffrin D, Tammeveski K (2004) Electrochem Commun 6:1
23. Kiema G, Aktay M, McDermott M (2003) J Electroanal Chem 540:7
24. Korshin G (1998) J Electroanal Chem 446:13
25. Premkumer J, Khoo S (2004) Electrochem Commun 6:984
26. Kiema G, Fitzpatrick G, Mcdermott M (1999) Anal Chem 71:4306
27. Dekanski A, Stevanovic J, Stevanovic R, Jovanovic V (2001) Carbon 39:1207
28. Ilangovan G, Pillai K (1997) J Electroanal Chem 431:11
29. Saleh M, Awad M, Okajima T, Suga K, Ohsaka T (2007) Electrochim Acta 52:3095
30. Engstrom R, Strasser V (1984) Anal Chem 56:136
31. Dekanski A, Stevanovic J, Stevanovic R, Nikolic B, Jovanovic V (2001) Carbon 39:1195
32. Premkumar J, Khoo S (2005) J Electroanal Chem 576:105
33. Theodoridou E, Besenhard J, Fritz H (1981) J Electroanal Chem 122:67
34. Sundberg K, Smyrl W, Atanasoska L, Atanasoska R (1989) J Electrochem Soc 136:434
35. Lee W, Lee J (2001) Appl Surf Sci 171:136
36. Moulder J, Stickle W, Sobol O, Bomben K (1992) In: Chastain J (ed) Handbook of X-ray photoelectron spectroscopy. Perkin-Elmer, Eden Prairie, MN
37. Yumitori S (2000) J Mater Sci 35:139
38. Beccat P, Da Silva P, Huibon Y, Kasztelan S (1999) Oil Gas Sci Technol 54:487
39. Mamantov G, Freeman D, Miller F, Zittel H (1965) J Electroanal Chem 9:305
40. Sullivan M, Kotz R, Haas O (2000) J Electrochem Soc 147:308
41. Nahle A, Reade G, Walsh F (1995) J Appl Electrochem 25:450
42. Grau J, Bisang J (2003) J Chem Technol Biotechnol 78:1032
43. Bazan J, Bisang J (2004) J Appl Electrochem 34:501